processes

MDPI

Article

Competitive Effect of Zinc and Cadmium on the Biosorption of Chromium by Orange Waste

Ana Belén Pérez-Marín, Juan Francisco Ortuño, María Isabel Aguilar *, Mercedes Lloréns and Víctor Francisco Meseguer

Departamento de Ingeniería Química, Facultad de Química, Universidad de Murcia, Campus de Espinardo, 30100 Murcia, Spain; abelenpm@um.es (A.B.P.-M.); jfortuno@um.es (J.F.O.); llorens@um.es (M.L.); vzapata@um.es (V.F.M.)

* Correspondence: maguilar@um.es; Tel.: +34-868887091

Abstract: Batch experiments were conducted to test orange waste (OW), an agricultural solid waste byproduct from the orange juice manufacturing industry, as adsorbent for binary solutions of Cd^{2+}-Cr^{3+} and Zn^{2+}-Cr^{3+}. Fourier transform infrared spectroscopy (FTIR) and the point of zero charge (pH_{pzc}) were used to identify the functional groups on the OW surface involved in biosorption. The biosorption equilibrium data for both binary-metal solutions were obtained and fitted to various isotherm models. The extended Sips and the non-modified Redlich-Peterson isotherm models gave the best fit for the experimental data. According to the extended Sips model, the maximum biosorption capacity of OW was 0.573 mmol·g^{-1} for Cd^{2+}, 0.453 mmol·g^{-1} for Zn^{2+}, and 1.96 mmol·g^{-1} for Cr^{3+}. The sorption capacity dropped to 0.061 mmol·g^{-1} for Cd^{2+} and to 0.101 mmol·g^{1} for Zn^{2+} in their binary systems with Cr^{3+} for the higher initial metal concentrations in the solution. However, the maximum sorption capacity of chromium was only slightly affected by the presence of Cd^{2+} or Zn^{2+}. For both binary systems, the presence of a second metal ion in the solution always conduces to a reduction in the sorption of the other metal in the solution. The presence of Cr^{3+} decreased the sorption of Cd^{2+} and Zn^{2+} more than vice versa. Conclusively, effective removal of Cr^{3+} ions from an aqueous solution can still be achieved in the presence of Cd^{2+} or Zn^{2+}.

Keywords: competitive biosorption; heavy metals; binary system; isotherm models; orange waste

Citation: Pérez-Marín, A.B.; Ortuño, J.F.; Aguilar, M.I.; Lloréns, M.; Meseguer, V.F. Competitive Effect of Zinc and Cadmium on the Biosorption of Chromium by Orange Waste. *Processes* **2024**, *12*, 148. https://doi.org/10.3390/pr12010148

Academic Editor: Antoni Sanchez

Received: 19 November 2023
Revised: 3 January 2024
Accepted: 4 January 2024
Published: 8 January 2024

1. Introduction

The pollution of water with heavy metals is a problem of global concern. Heavy metals can have strong toxic effects even when they are present at low concentrations. They can also accumulate in the food chain and, due to their solubility and their mobility, can cause serious health and ecological problems [1]. Chromium can cause nausea, diarrhoea, dermatitis, kidney and liver damage, internal and respiratory problems [2,3]. Zinc may cause loss of appetite, nausea, irritability and muscle stiffness [4]. Symptoms of cadmium toxicity include anaemia, hypertension, and renal dysfunction. The kidneys may be considered as the critical target organ following ingestion [4,5].

Cadmium, zinc, and chromium are widely used in many industrial activities such as electroplating, leather tanning, nuclear power plants, pigment production, and the fertilizer and textile industries. Therefore, these metals are usually present in the effluents of these industries. Cadmium and zinc can exist under one oxidation state. Although chromium can exist under six oxidation states and the most important ones in water are trivalent Cr(III) and hexavalent Cr(VI) [6]. Due to the greater toxicity of Cr(VI), the removal of Cr (VI) from aqueous effluents has been further investigated. However, Cr(III) ions can easily be oxidized to Cr(VI) in the presence of oxidizing agents and therefore their removal from aqueous effluents is also highly important [7]. Furthermore, to ensure proper management of wastewater treatment plants to prevent this compound from reaching the

aquatic environment, it is necessary to protect the functions performed by the microorganisms present in activated sludge [8]. The European Chemicals Agency (ECHA) has, for registered substances (REACH), established a parameter called $PNEC_{STP}$ (predicted non effect concentration for microorganism present in sewage), which can be used as a toxicity value to assess the risk for microbial activity in wastewater treatment plants. The $PNEC_{STP}$ value for the compound used to prepare the Cr(III) stock solution is 2.29 $mg \cdot L^{-1}$.

Current technologies, including ion exchange, precipitation, solvent extraction, and membrane-based processes, have some limitations in terms of their economic and/or technical feasibility for the removal of heavy metals from industrial wastewater [9–11]. Therefore, the search for efficient and cost-effective technologies for the removal of heavy metals from water has led to an increased focus on the use of biological materials as biosorbents. Biosorption has been recognized as an alternative technology to replace the above mentioned technologies [10,12,13].

Worldwide, agricultural wastes are mostly disposed of by dumping or incineration, which contributes negatively to environmental pollution and also neglects the potential of these wastes [14,15]. Recent studies have proposed agricultural wastes as ideal adsorbents for the removal of heavy metals from wastewater. Agricultural wastes such as apricot pits [16], rice straw [17], OW [18], walnut shells [19], cocoa [20], and banana peels [21,22] have shown promising results for heavy metals biosorption.

Most biosorption research has been focused on the uptake of single metal species from aqueous effluents and little attention has been paid to the study of simultaneous metal removal in multi-metal systems [23]. However, under most conditions, aqueous streams contain several types of metal ions simultaneously [24]. When several metal ions are present in the water, competition phenomena for the adsorption sites may occur. Therefore, it is of great importance to understand the behavior of metal ion mixtures, by studying the effect that the presence of one metal has on the uptake of other metal ions [24,25].

Furthermore, the equilibrium modelling of biosorption in multicomponent systems, an essential aspect in designing treatment systems, has received inadequate attention [26]. Therefore, it is necessary to examine the process of removing multiple metals from solutions, at least binary ones [27], by obtaining the equilibrium isotherms in multicomponent systems [28–31].

Cadmium, zinc, and chromium are three widely used metals that often occur simultaneously in metal-bearing industrial effluents. In this context, the present work aims to study the equilibrium isotherm of two binary systems (Cd^{2+}-Cr^{3+} and Zn^{2+}-Cr^{3+}) using OW as a biosorbent. Several multicomponent sorption models, commonly used to correlate multicomponent equilibrium data, were used to describe the experimental data obtained for the binary systems studied. In addition, Fourier transform infrared spectroscopy (FTIR) of the biomass, before and after metals sorption, and the determination of the biomass point of zero charge (pH_{pzc}) were used to identify the functional groups on the OW surface involved in biosorption.

The research developed in this work can contribute to the achievement of Sustainable Development Goal (SDG) 6 of the 2030 Agenda for Sustainable Development: "Ensure availability and sustainable management of water and sanitation for all" [8].

Specifically, it aligns with target 6.3 because it will contribute to improving water quality by reducing pollution caused by the release of heavy metals into aquatic systems and increasing water reuse.

At the same time, it will enable the protection and restoration of water-related ecosystems (target 6.6).

2. Materials and Methods

2.1. Adsorbent Preparation

The OW used as an adsorbent was provided by an orange juice company located in Murcia (Spain). The OW was first cut into small pieces and extensively washed with tap water to remove adhering dirt and soluble components such as reducing sugars, resins,

tannins, and coloring agents. The OW was then oven-dried to a constant weight, at 50–60 °C. The washed and dried material was crushed and sieved to obtain particles measuring less than 1.5 mm in size [18,32–34].

2.2. Chemical

Single metal synthetic stock solutions (2000 $mg \cdot L^{-1}$) of chromium, cadmium, and zinc were prepared by dissolving the accurately weighed amounts of $Cr(NO_3)_3 \cdot 9H_2O$, cadmium metal, and zinc metal (analytical grade), respectively, in 100 mL of distilled water and 10 mL of concentrated nitric acid and diluted with distilled water to obtain one liter of each solution. Experimental binary metal solutions were prepared by mixing and diluting, with distilled water, the appropriate volume of stock solutions to obtain the desired metal concentrations of each metal in the binary mixture.

All chemicals used were purchased from Panreac and were of analytical reagent grade.

2.3. Adsorbent Characterization

Fourier transform infrared spectroscopy (FTIR) and the point of zero charge (pH_{pzc}) were determined to characterize the OW used as biosorbent.

FTIR analysis of raw OW and FTIR analysis of OW after metal loading were carried out to find out which functional groups are responsible for metal ion sorption. FTIR spectra were obtained using a Fourier transform infrared spectroscope (Model: Perkin Elmer 16F PC; Perkin Elmer España, S.L., Madrid, Spain) with a KBr salt as the spectroscopic window. The FTIR optical system has a resolution of 4 cm^{-1}. The instrument is equipped with a deuterated triglycine sulphate (DTGS) detector. Spectra were collected over the range from 4000 cm^{-1} to 500 cm^{-1}.

pH_{pzc} was obtained to determine the pH at which the OW, immersed in an electrolyte, has a net zero electrical charge on its surface [35].

An amount of 50 mL of 0.01 M NaCl solution was placed in different 100 mL Erlenmeyer flasks and the pH of each solution was adjusted between 1 and 9 by adding the appropriate amounts of dilute NH_4OH or HNO_3 solutions. Then, 0.2 g of OW biomass was added to each Erlenmeyer. After 48 h of stirring at room temperature, the final pH values were measured. The pH_{pzc} was calculated by plotting the variation in pH values against the initial pH. The point where the variation in pH is zero corresponds with the pH_{pzc}.

2.4. Biosorption Procedure

Batch uptake studies were performed, at constant room temperature, by contacting 0.2 g of OW (particle size < 1.5 mm) with 50 mL of the binary solutions (Cd^{2+}-Cr^{3+} or Zn^{2+}-Cr^{3+}) in 100 mL Erlenmeyer flasks. The initial metal concentrations in the binary solutions ranged from 0 $mmol \cdot L^{-1}$ to 5.8 $mmol \cdot L^{-1}$. The mixture was stirred magnetically for 3 days. This time is more than sufficient to ensure that equilibrium has been reached. The pH was continuously adjusted to 4 by using small volumes of dilute NH_4OH or HNO_3 solutions. After the established contact time, the samples were filtered through glass fiber prefilters (Millipore AP40; Millipore Iberica SA, Madrid, Spain). The filtrates were analyzed for residual metal ion concentration by atomic absorption spectrophotometry using an air—acetylene flame (Perkin Elmer model AA300; PerkinElmer Inc., Waltham, MA, USA). All experiments were performed in duplicate. The experimental conditions were established according to results obtained in previous studies carried out to optimize the biosorption of Cd^{2+}, Zn^{2+}, and Cr^{3+} by OW in mono-adsorbate systems [18,32,33].

The uptake of each metal in the binary system at equilibrium was calculated using the general definition:

$$q_{e,Me} = \frac{C_{0,Me} \cdot V_0 - C_{e,Me} \cdot V_e}{m} \quad (1)$$

where $C_{0,Me}$ and $C_{e,Me}$ are the metal concentrations in the solution ($mmol \cdot L^{-1}$) at time 0 and at equilibrium, respectively, V_0 and V_e are the solution volumes (L) at time 0 and at equilibrium, respectively, and m is the mass of the biosorbent used (g).

The selectivity of OW for Cd^{2+}, Zn^{2+}, and Cr^{3+} in the binary mixtures was evaluated in terms of individual biosorption efficiency (Yi, %), relative metal i biosorption (Ri, %) and relative coverage (θ_i, %) [36]. These terms are defined as follows:

$$Y_i(\%) = \frac{C_{0,Mei} - C_{e,Mei}}{C_{0,Mei}} \cdot 100 \quad (2)$$

$$R_i(\%) = \frac{q_{e,Mei}\ \text{binary system}}{q_{e,Mei}\ \text{monoadsorbate system}} \cdot 100 \quad (3)$$

$$\theta_i(\%) = \frac{q_{e,Mei}}{\sum_{j=1}^{j=n} q_{e,Mej}} \cdot 100 \quad (4)$$

2.5. Adsorption Models

The distribution of the metal ions between the liquid phase and the sorbent, once at equilibrium, can usually be expressed by a series of isotherms. In the present work, experimental isotherms were obtained, and several models were used to describe the experimental equilibrium data (Table 1). These models have previously been used in others works to describe the equilibrium in multi-adsorbate systems [23,29,37–39].

Table 1. Multi-adsorbate sorption isotherms.

Isotherm Model	Parameters
Extended Langmuir isotherm [18,32,33] $q_{e,Mei} = \frac{q_{max} \cdot b_{Mei} \cdot C_{e,\ Mei}}{1+\sum_{j=1}^{N} b_{Mej} \cdot C_{e,\ Mej}}$	q_{max}: maximum sorption capacity ($mmol \cdot g^{-1}$) b_{Mei} and b_{Mej} affinity constant of the biomass for metals i and j, respectively ($L \cdot mmol^{-1}$); $q_{max,Mei}$: maximum sorption capacity for metal i ($mmol \cdot g^{-1}$); η_{Mei} and η_{Mej}: modified Langmuir coefficient for metals i and j, respectively.
Non-modified Langmuir isotherm [23,29,38,39] $q_{e,Mei} = \frac{q_{max,Mei} \cdot b_{Mei} \cdot C_{e,\ Mei}}{1+\sum_{j=1}^{N} b_{Mej} \cdot C_{e,\ Mej}}$	
Modified Langmuir isotherm [37,38,40,41] $q_{e,Mei} = \frac{q_{max,Mei} \cdot b_{Mei} \cdot \frac{C_{e,\ Mei}}{\eta_{Mei}}}{1+\sum_{j=1}^{N} b_{Mej} \cdot \frac{C_{e,\ Mej}}{\eta_{Mej}}}$	
Extended Sips isotherm [29,37,41] $q_{e,Mei} = \frac{q_{max,Mei} \cdot b_{Mei} \cdot C_{e,\ Mei}^{\frac{1}{n_i}}}{1+\sum_{j=1}^{N} b_{Mej} \cdot C_{e,\ Mej}^{\frac{1}{n_j}}}$	$q_{max,Mei}$: maximum sorption capacity for metal i ($mmol \cdot g^{-1}$); b_{Mei} and b_{Mej}: affinity constant of the biomass for metals i and j, respectively ($L^{1/ni} \cdot mmol^{-1/ni}$); n_i and n_j: measure of heterogeneity of binding surface for metals i and j, respectively.
Non-modified Redlich–Peterson isotherm [18,32,33] $q_{e,Mei} = \frac{K_{RPi} \cdot C_{e,\ Mei}}{1+\sum_{j=1}^{N} \alpha_{RPj} \cdot C_{e,\ Mej}^{\beta j}}$	K_{RPi} ($L \cdot g^{-1}$) and α_{RPj} ($L^{\beta j} \cdot mmol^{-\beta j}$): R-P equilibrium constants for metals i and j, respectively; B_j: R-P isotherm exponent for metal j.
Sheindorf–Rebuhn–Sheintuch (SRS) isotherm [18,32,33] $q_{e,Mei} = K_{Fi} \cdot C_{e,\ Mei} \cdot \left(\sum_{j=1}^{N} \alpha_{ij} \cdot C_{e,\ Mej} \right)^{(\frac{1}{n_i})-1}$	K_{Fi}: constant of the Freundlich model ($L \cdot g^{-1}$); n_i: Freundlich constant related with the intensity of sorption; α_{ij} ($L \cdot mmol^{-1}$): SRS constant that represents the inhibitory effect of component i on the adsorptive removal of component j.

$q_{e,Mei}$: amount of Me*i* adsorbed at equilibrium ($mmol \cdot g^{-1}$); $C_{e,Mei}$ and $C_{e,Mej}$: residual concentrations of metal i and j at equilibrium, respectively ($mmol \cdot L^{-1}$).

2.6. Statistical Analysis

The experimental data were fitted to the different models using the nonlinear fitting facilities of the Solver add-in to Microsoft Excel. The validity of the models was evaluated using the average relative error (ARE, %) function, which measures the relative differences between the experimental data and those predicted by the models.

The average relative error was developed by Marquardt [42] with the aim of minimizing the fractional error distribution over the whole concentration range and is widely used in the literature [43]. It is given by the expression:

$$\text{ARE}\ (\%)\ = \frac{100}{n}\sum_{i=1}^{N}\left|\frac{q_{e,cal} - q_{e,exp}}{q_{e,exp}}\right| \quad (5)$$

where $q_{e,exp}$ (mmol·g^{-1}) is the experimental adsorption capacity at equilibrium, $q_{e,cal}$ (mmol·g^{-1}) is the calculated adsorption capacity at equilibrium.

3. Results and Discussion

3.1. Orange Waste Characterization

3.1.1. FTIR Spectra

Figure 1 shows FTIR spectra of OW samples before and after the biosorption process. The complex nature of the material can be observed from the high number of adsorption peaks. As can be seen, the FTIR spectra before and after metal adsorption are very similar. Only slight shifts in the wavenumber corresponding to some peaks can be observed.

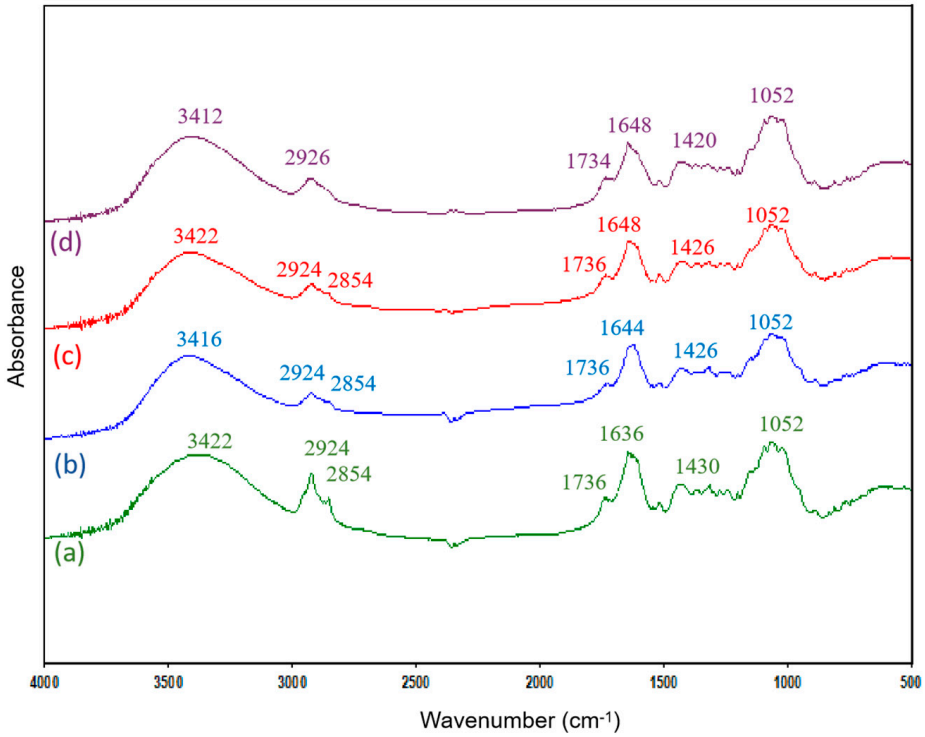

Figure 1. FTIR spectra of OW: (a) raw OW, (b) OW loaded with cadmium, (c) OW loaded with zinc, and (d) OW loaded with chromium.

The broad peak at 3422 cm^{-1} can be attributed to O–H stretching vibrations of free hydroxyl groups (alcohols and phenols) and bonded OH bands of carboxylic acids present in the main components of OW (cellulose, pectin, hemicellulose, etc.) [34,35]. In addition, the amplitude and intensity of this peak may be related to the presence of adsorbed water molecules from atmospheric moisture [44,45]. To minimize this effect, the analyzed samples were dried in an oven and stored in a desiccator prior to its use. The peak at 2924 cm^{-1} was recognized as symmetric or asymmetric –CH stretching of the aliphatic groups, and the peak at 2853 cm^{-1} can be associated with symmetric stretching vibration of these groups [45]. The peak at 1736 cm^{-1} shows the stretching vibration of the C=O bond due to non-ionic carboxyl groups, and may be assigned to carboxylic acids or their esters (–COOH, –$COOCH_3$) [46]. The peak around 1636 cm^{-1} is due to the C=C stretching that can be

attributed to the presence of aromatic rings, COO- asymmetric stretching, and the bending vibration of the interlayer water molecules [45]. These bands can reveal the presence of pectin, hemicellulose, and lignin in the OW [47].

The peak at 1431 cm^{-1} can be attributed to the symmetric stretching vibrations of C=O in ionic carboxylic groups (-COO−) [48] and to HCH and OCH in plane bending vibration (as in cellulose). The bands observed at 1052 cm^{-1} can be assigned to the C–O stretching of alcohols and carboxylic acids [49,50]. The 1000 cm^{-1}–1200 cm^{-1} finger print region shows the characteristic cellulose peaks [51,52], indicating cellulose as the main backbone of the material.

Shifts in the peak positions at 3422 cm^{-1}, 1636 cm^{-1}, and 1430 cm^{-1} were observed during metal sorption on OW, suggesting the possible involvement of the cited functional groups in the heavy metal sorption.

The changes in the intensity of the band at 3422 cm^{-1} and at 1636 cm^{-1} would be due to the different amount of water adsorbed. Cai et al., 2023 [53], who studied the FTIR spectra of biochar obtained at different pyrolysis temperatures, observed a decrease in the intensity of the peak at 3425 cm^{-1} with increasing pyrolysis temperature, indicating the dehydration of the samples. On the other hand, the shift of this peak (especially in the sample after chromium sorption, to 3412 cm^{-1}), could be an indication that OH groups could be involved in metal adsorption.

The largest shift in absorption peaks occurs in the 1636 cm^{-1} band, which shift to 1644 cm^{-1}/1648 cm^{-1} after sorption, and the 1430 cm^{-1} band, which shifts to 1426 cm^{-1}/1420 cm^{-1}. Similar results were obtained by Lasheen et al., 2012 [48], who pointed out that the shift in the 1636 cm^{-1} band could be due to a change in the binding energy of carboxylate groups. Pereira de Carvalho, 2015 [54], studying the adsorption of methylene blue on banana peel, shows that some bands in the FTIR spectra are shifted after adsorption. Thus, the band at 1613.6 cm^{-1} shifted to 1622.9 cm^{-1}, indicating that the carbonyl group could be involved in the adsorption mechanism.

As has been reported by Ellerbrock and Gerke, 2021 [55], interactions between cations and organic matter occur mainly through functional groups containing double bonds between C and O atoms, such as carboxylate anions, carboxylic acids, esters, amides (proteins), aldehydes, and ketones. These groups are negatively charged (i.e., as carboxylate anions) or partially negatively charged (i.e., carboxylic acids, esters, amides, aldehydes, and ketones), which contributes to cation exchange, among other adsorption mechanisms. The shift of the maximum of the FTIR absorption bands as a result of the interaction with cations is related to changes in the bond strength within the C=O double bond. In several studies it was found that the addition of cations shifted the maximum of the COO- peak towards lower wave numbers, while in others it was found that the COO- peak shifted upwards.

The results obtained confirmed the involvement of carboxylic acids groups in the binding of metal ions by OW. Previous studies have also shown the important role played by carboxylic acid groups in the adsorption of metals on OW [33].

3.1.2. pH_{pzc} Test

The results of the experiments conducted to determine pH_{pzc} are shown in Figure 2. The pH_{pzc} obtained was ≈5.3, slightly acidic, indicating the acid character of the solid surface. The pK_a value of R–COOH, which seems to be the major OW functional group involved in heavy metal sorption, is in the range of 3.5–5.5 [46]. At pH values over 5.3, more functional groups are deprotonated, resulting in more negative binding sites and greater attraction of positively charged metal ions [56]. The assays were performed at pH 4, in accordance with the optimal experimental conditions determined in previous studies [18,32,33]. These results indicate that a mechanism other than electrostatic attraction must be involved in heavy metal sorption onto OW. Similar results were obtained by other researchers and other mechanisms have been proposed for heavy metal biosorption: complexation reaction, ion exchange, and precipitation [35,57–62]. Metal complexes are

formed by complexation reactions on the adsorbent surface when heavy metal ions interact with oxygenated functional groups such as carboxyl, hydroxyl, and phenolic groups that are present on the sorbent surface. In ion exchange, metals in solution displace protons from oxygen-containing functional groups and other exchangeable cations, such as Na^+, K^+, Ca^{2+} and Mg^{2+}, present on the sorbent surface. Finally, precipitation involves the formation of mineral precipitates on the surface of the sorbent [63,64].

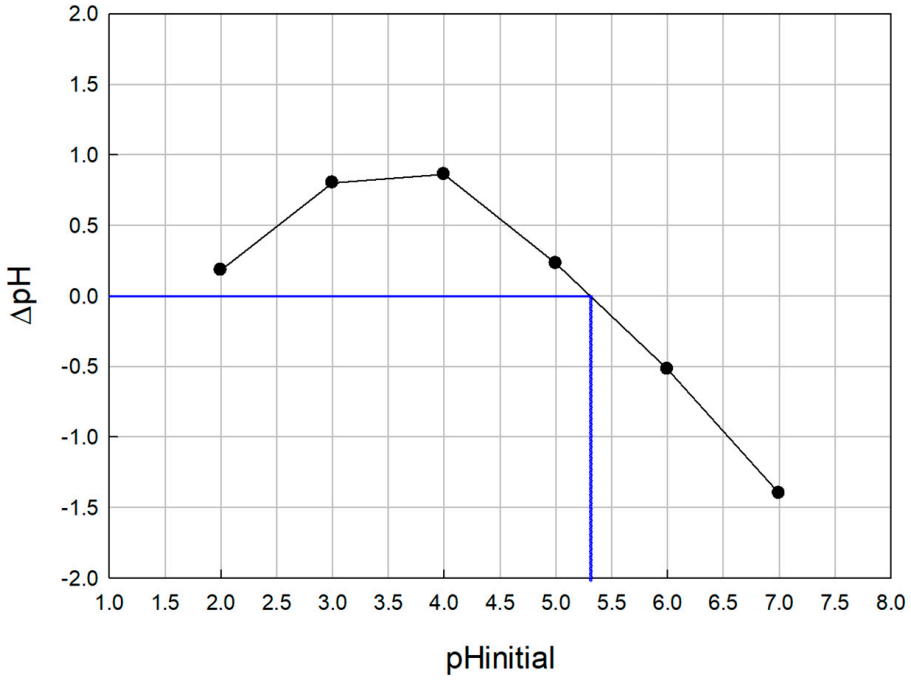

Figure 2. Representation for the pH_{pzc} of OW determination (the blue line indicates pH_{pzc}: pH at which ΔpH = 0).

As shown by FTIR analysis, the surface of OW has oxygenated functional groups (carboxyl, hydroxyl, phenolic) which are responsible for the removal of metals through the formation of surface metal complexes and ionic exchange between the metals and protons from these functional groups. Furthermore, the metals can also be exchanged with other cations present on the surface of the OW. The concentrations of the main cations on OW were determined in a previous study [33]. According to these results, OW contains 0.229 mmol $Na^+ \cdot g^{-1}$, 0.005 mmol $K^+ \cdot g^{-1}$, 0.577 mmol $Ca^{2+} \cdot g^{-1}$, and 0.122 mmol $Mg^{2+} \cdot g^{-1}$. These results suggest that the surface complexation of heavy metals and their ionic exchange with major cations and with protons may be the main mechanisms of biosorption [63,65].

3.2. Experimental Sorption Equilibrium Data Analysis for the Cd^{2+}-Cr^{3+}, and Zn^{2+}-Cr^{3+} Binary Systems

The competitive adsorption isotherms on OW are shown in Figures 3 and 4 for the binary systems Cd^{2+}-Cr^{3+} and Zn^{2+}-Cr^{3+}.

The uptake of each one of the metals studied increased with increases in their initial solution concentration and, although the isotherms slopes decreased at higher solution concentrations, sorbent saturation is clearly not reached in any case. The presence of co-ions decreased the sorption capacity and this effect increased with increasing initial co-ion concentration. The suppressive effect of chromium ions on cadmium and zinc adsorption was much greater than the effect of cadmium and zinc ions on chromium adsorption.

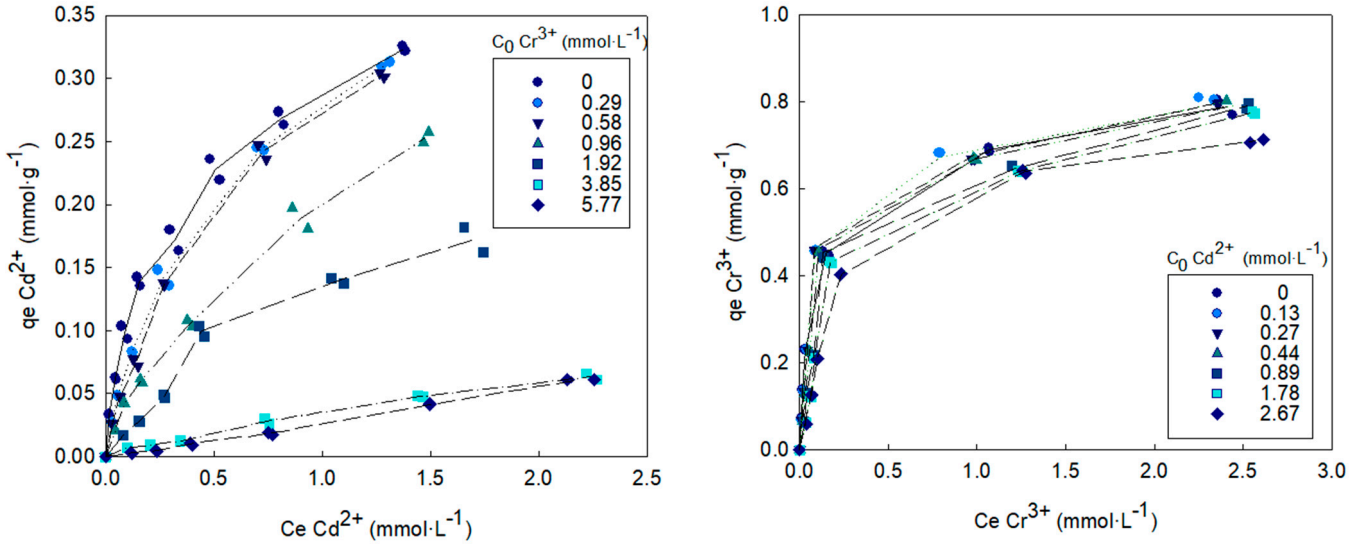

(**a**) (**b**)

Figure 3. Metal A biosorption isotherm in the presence of metal B co-ions. (**a**) Metal A = Cd^{2+} and metal B = Cr^{3+}, (**b**) Metal A = Cr^{3+} and metal B = Cd^{2+}.

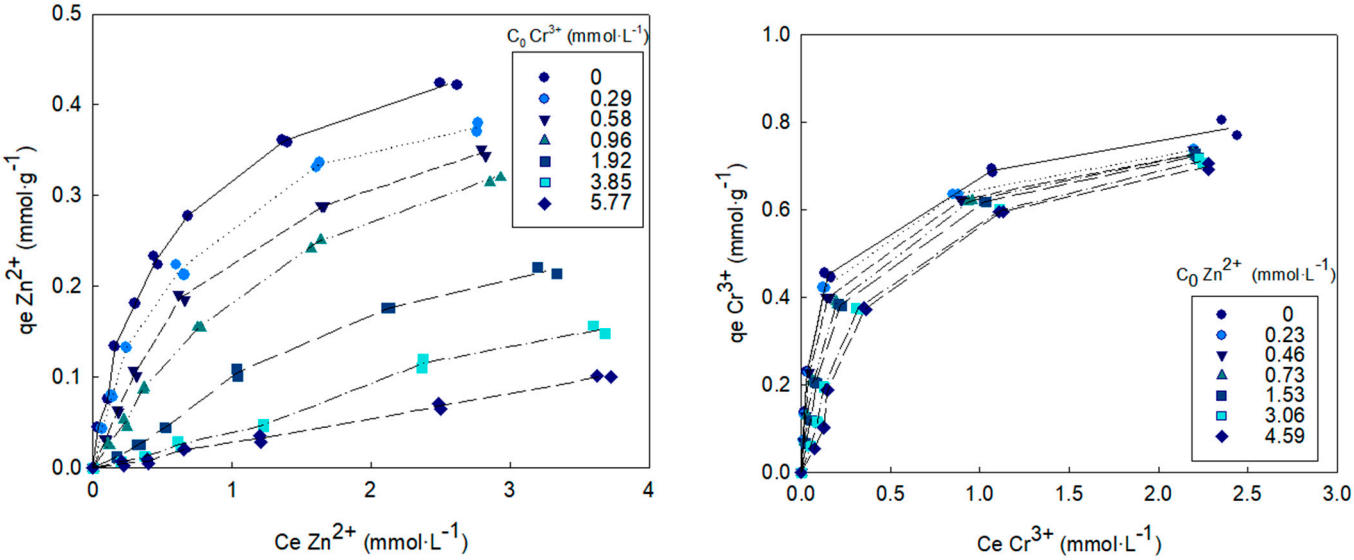

(**a**) (**b**)

Figure 4. Metal A biosorption isotherm in the presence of metal B co-ions. (**a**) Metal A = Zn^{2+} and metal B = Cr^{3+}, (**b**) Metal A = Cr^{3+} and metal B = Zn^{2+}.

Similar results were obtained by Kim, 2003 [66]. This study concluded that Cr^{+3} and Pb^{+2} ions had a strong inhibitory effect on the removal of Cd^{+2} and that the presence of Cd^{+2} had little effect on the removal of both Pb^{+2} and Cr^{+3} in binary solutions. Similarly, Ma and Tobin, 2003 [67], concluded in their study that chromium and copper co-ions caused large and similar reductions in cadmium uptake while the effect of cadmium on chromium and copper uptake was smaller.

The selectivity of OW for cadmium, zinc, and chromium in the binary mixtures, Cd^{2+}-Cr^{3+} and Zn^{2+}-Cr^{3+}, was evaluated in terms of the metal i relative biosorption, the individual biosorption efficiency, and the relative coverage. Figures 5–7 show, as an example, the variation in these parameters with different initial concentrations of Cd^{2+} and Cr^{3+} in the binary system Cd^{2+}-Cr^{3+}. Similar results were obtained for the binary system Zn^{2+}-Cr^{3+} (Supplementary Material: Figures S1–S3).

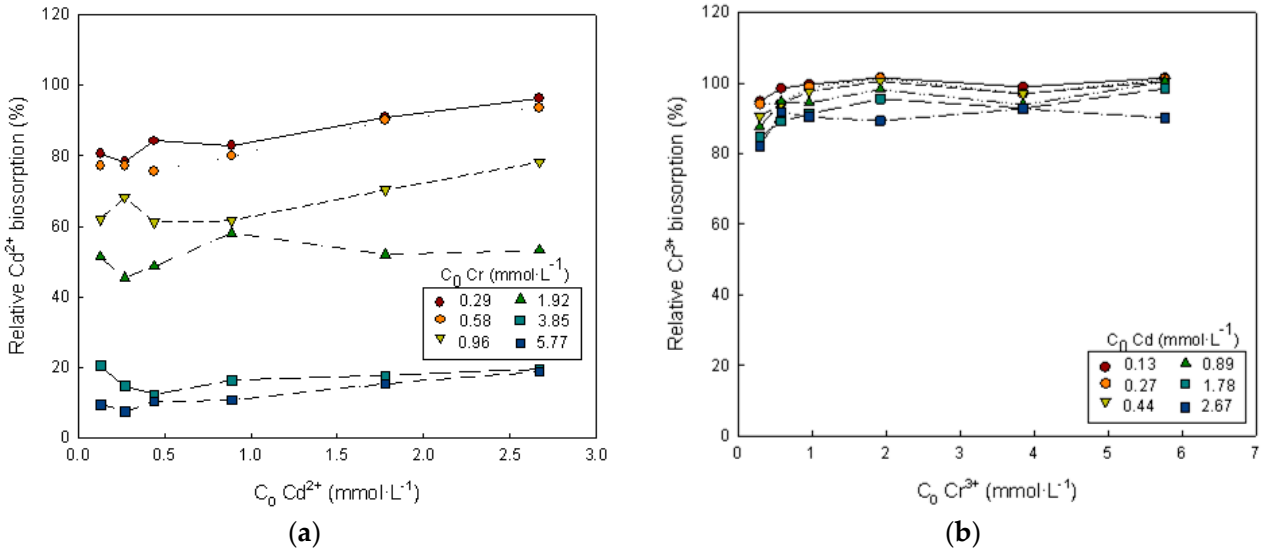

Figure 5. Dependence of the relative metal i biosorption on the initial concentrations of metals i and k. (**a**) Metal $i = Cd^{2+}$ and metal $k = Cr^{3+}$, (**b**) metal $i = Cr^{3+}$ and metal $k = Cd^{2+}$.

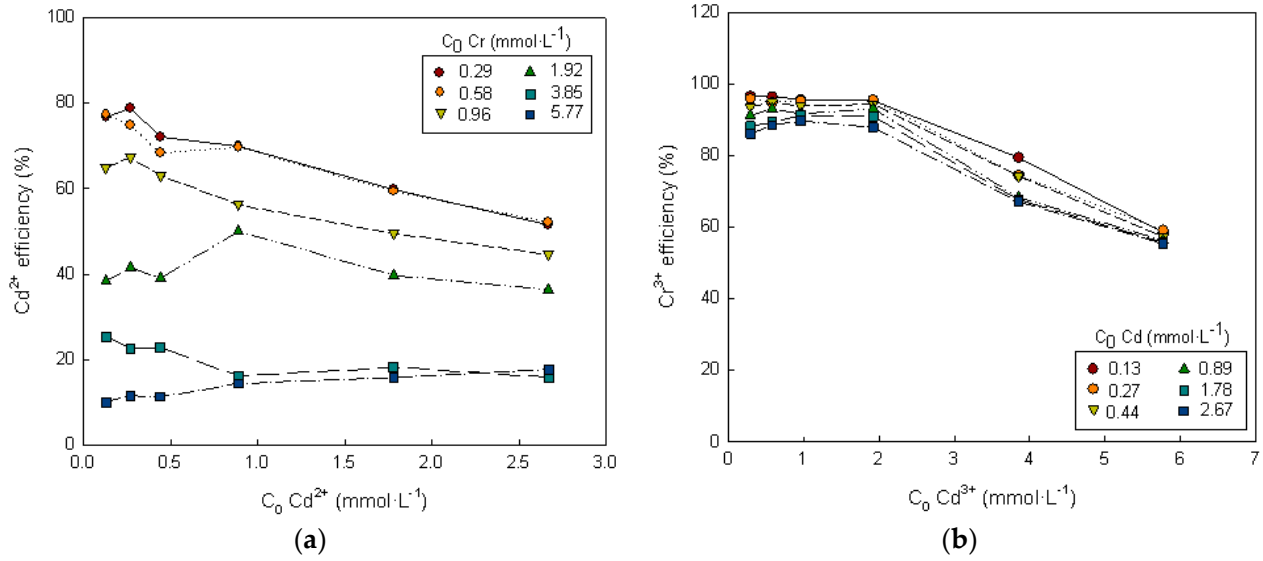

Figure 6. Dependence of the biosorption efficiency of metal i on the initial concentrations of metals i and k. (**a**) Metal $i = Cd^{2+}$ and metal $k = Cr^{3+}$, (**b**) metal $i = Cr^{3+}$ and metal $k = Cd^{2+}$.

The values of relative cadmium biosorption appreciably below 100% (Figure 5) indicate that its biosorption has been significantly reduced by the presence of chromium ions in the solution. The higher the initial chromium concentration, the lower the cadmium biosorption. When the initial concentration of chromium in the solution was 5.77 mmol·L^{-1}, the cadmium biosorption capacity was only 19% of its original value without chromium competition. The relative cadmium biosorption increased when the initial cadmium concentration, or the ratio of the cadmium concentration to total metal ions concentration, were increased. Relative chromium biosorption values close to 100% indicate that chromium biosorption was not greatly affected by the presence of cadmium ions. It can be noted that, for the highest initial cadmium concentration tested in the binary solution, the chromium biosorption capacity remained at 92% of its original capacity without cadmium competition (Figure 5).

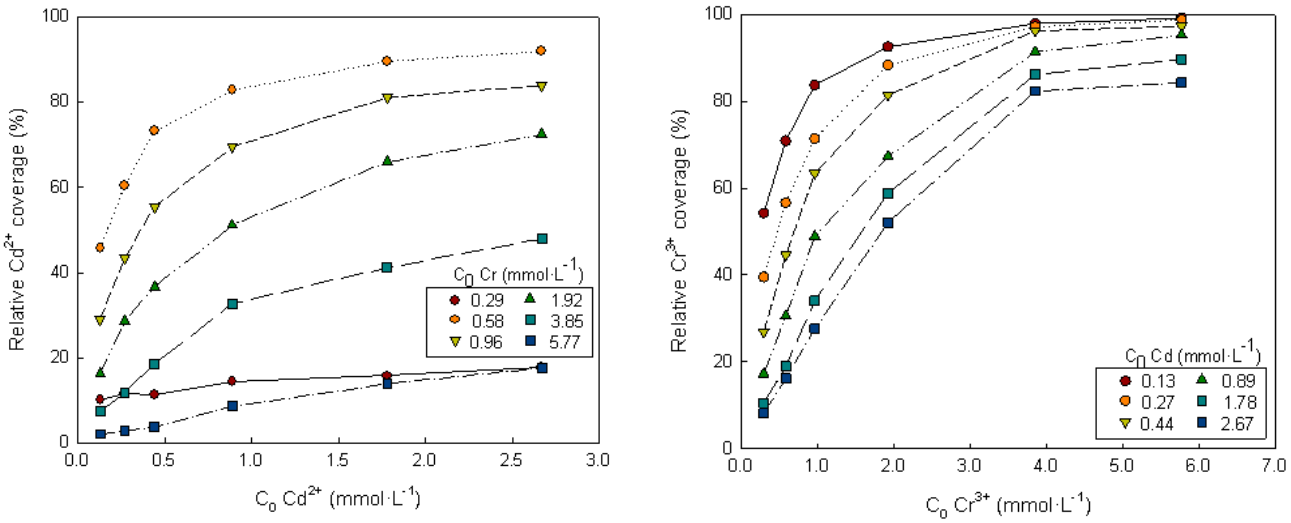

Figure 7. Dependence of the relative metal i coverage on the initial concentrations of metals i and k. (**a**) Metal $i = Cd^{2+}$ and metal $k = Cr^{3+}$, (**b**) metal $i = Cr^{3+}$ and metal $k = Cd^{2+}$.

Similar results were obtained in the Zn^{2+}-Cr^{3+} binary system. Zinc uptake was greatly reduced by the presence of chromium (zinc biosorption capacity remained only 24% of its original capacity when the initial concentration of chromium in solution were 5.77 mmol·L^{-1}), while chromium biosorption capacity remained at 89% of its original capacity for the highest zinc concentration tested in the binary solution.

Values of relative metal biosorption lower than 100%, in both binary systems studied, clearly confirm the antagonistic effects since competitive adsorption is important. Similar results have been reported in the literature for the adsorption of mixtures of the studied heavy metals by different adsorbents [13,24,68–70].

As can be seen in Figure 6, the biosorption efficiency of each metal decreased as the initial metal concentration increased. The biosorption efficiency was in the order $Y(Cr^{3+}) > Y(Cd^{2+})$ (Figure 6). Similar results were obtained in the Zn^{2+}-Cr^{3+} binary system; the biosorption efficiency was in the order of $Y(Cr^{3+}) > Y(Zn^{2+})$.

For each metal in the binary solution, the relative coverage of a metal (metal *i*) increases as its initial concentration increases and as the concentration of the other metal in solution (metal *k*) decreases. The relative coverage of cadmium is more influenced by the presence of chromium than vice versa (Figure 7). The same results were observed for the binary system Zn^{2+}-Cr^{3+} (Supplementary Material: Figure S2).

It is not easy to find a standard that allows us to determine how the properties of the metals affect the biosorption selectivity. The preference of biomass for a specific metal does not depend only on the chemical and physical properties of the metals. The final behavior is the result of a combination of the specific surface properties of the biosorbent, the physicochemical parameters of the solution, and the chemical and physical properties of the metals. For the biosorption of heavy metals, and taking into account the metal properties, it can be observed that the affinity of the biomass is higher at higher ionic charges. Additionally, the adsorption of metal ions on the biosorbent surface is favored by the reduction in the hydrated ionic radius [71], which facilitates access to the adsorbent surface active sites and ion exchange with the adsorbent's exchangeable cations. The behavior of metal ions tested in this work followed the aforementioned trend as a function of the ionic radius (Table 2), [72] with adsorption following the order chromium > zinc > cadmium; charge: Cd^{2+}, Zn^{2+}, $Cr(OH)^{2+}$ andCr^{3+}. Similar conclusions have been obtained by other authors [71,73].

Table 2. Hydrated ionic radii for the heavy metals studied.

Element	Cadmium	Zinc	Chromium
Hydrated ionic radus (Å)	0.96	0.74	0.62

3.3. Modeling of Metal Biosorption from Binary Solutions Using Multicomponent Adsorption Isotherms

The equilibrium biosorption data of the two binary systems studied were analyzed using different binary isotherm models [23,28,31,61,67,74–77]: extended Langmuir, non-modified Langmuir, modified Langmuir, extended Sips, non-modified Redlich–Peterson, and Sheindorf–Rebuhn–Sheintuch isotherms (Table 1).

The values of uptake and residual solution concentrations of both metals, once equilibrium was reached attained, were used to evaluate the parameters of the different isotherms. The values of these characteristic parameters for each one of the isotherm models listed in Table 1 were obtained by non-linear regression and are summarized in Table 3. The average relative errors are also shown, providing a measure of the goodness of fit of each model.

The obtained average errors of the fitting to the different isotherm models tested varied between 16.7% and 47%. With the exception of the Sheindorf–Rebuhn–Sheintuch isotherm model, no great differences were obtained between the fitting of binary experimental data to the models employed (ARE between 16.7% and 20.3%), although the best description of the experimental data was provided by the extended Sips isotherm and the non-modified Redlich–Peterson isotherm. The close relationship between the experimental sorption capacity data and those data provided by the extended Sips model, for the two binary systems studied, can be observed in Figure 8.

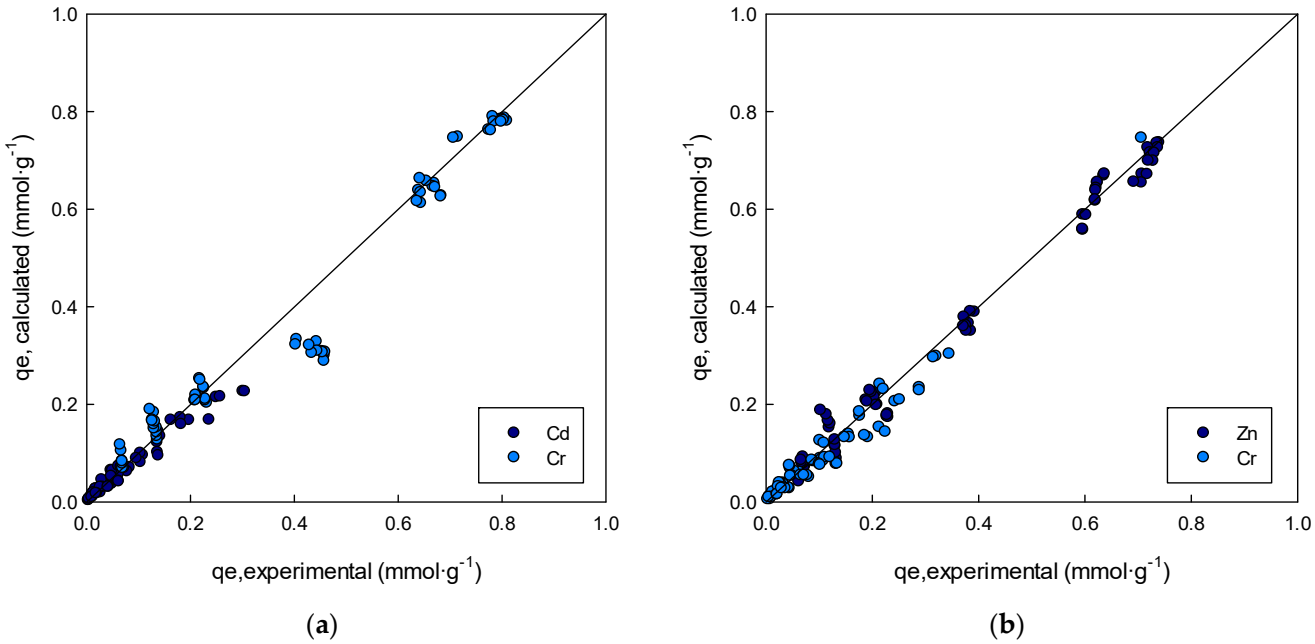

Figure 8. Relationship between the experimental sorption capacity data and sorption capacity data provided by the extended Sips model (**a**) Cd-Cr system, (**b**) Zn-Cr system.

Other researchers found the best description of the experimental equilibrium data of their studies with the extended Sips model [29,78]. This model is suitable for predicting adsorption on heterogeneous surfaces, thus avoiding the limitation of increasing adsorbate concentration normally associated with the Freundlich model [79]. Therefore, at low adsorbate concentrations, this model reduces to the Freundlich model, but at high adsorbate concentrations, it predicts the Langmuir model (monolayer adsorption).

Table 3. Characteristic parameters of each one of the studied isotherm models for the biadsorbate sorption and average relative errors of the fits.

		Cd^{2+}-Cr^{3+} $Me_1 = Cd^{2+}$, $Me_2 = Cr^{3+}$	Zn^{2+}-Cr^{3+} $Me_1 = Zn^{2+}$, $Me_2 = Cr^{3+}$
Extended Langmuir isotherm	q_{max} ($mmol \cdot g^{-1}$)	0.755	0.58
	b_{Me1} ($L \cdot mmol^{-1}$)	0.698	20.32
	b_{Me2} ($L \cdot mmol^{-1}$)	9.39	0.733
	ARE (%)	19.37	7.79
Non-modified Langmuir isotherm	$q_{max,Me1}$ ($mmol \cdot g^{-1}$)	0.430	0.512
	b_{Me1} ($L \cdot mmol^{-1}$)	1.47	0.905
	$q_{max,Me2}$ ($mmol \cdot g^{-1}$)	0.779	0.775
	b_{Me2} ($L \cdot mmol^{-1}$)	10.27	8.08
	ARE (%)	18.20	19.78
Modified Langmuir isotherm	$q_{max,Me1}$ ($mmol \cdot g^{-1}$)	0.430	0.523
	b_{Me1} ($L \cdot mmol^{-1}$)	1.31	0.90
	η_{Me1}	0.895	1.01
	$q_{max,Me2}$ ($mmol \cdot g^{-1}$)	0.779	0.773
	b_{Me2} ($L \cdot mmol^{-1}$)	10.24	8.04
	η_{Me2}	0.997	0.99
	ARE (%)	18.20	19.78
Extended Sips isotherm	$q_{max,Me1}$ ($mmol \cdot g^{-1}$)	0.573	0.453
	b_{Me1} ($L^{1/nMe1}$ $mmol^{-1/nMe1}$)	1.30	2.31
	n_{Me1}	0.889	0.575
	$q_{max,Me2}$ ($mmol \cdot g^{-1}$)	1.096	0.787
	b_{Me2} ($L^{1/nMe2}$ $mmol^{-1/nMe2}$)	14.39	12.78
	n_{Me2}	0.840	1.00
	ARE (%)	16.75	19.04
Non modified Redlich–Peterson isotherm	$K_{RP,Me1}$ ($L \cdot g^{-1}$)	1.33	0.747
	$\alpha_{RP,Me1}$ ($L^{\beta 1} \cdot mmol^{-\beta 1}$)	3.73	1.49
	β_{Me1}	0.430	0.621
	$K_{RP,Me2}$ ($L \cdot g^{-1}$)	16.72	10.03
	$\alpha_{RP,Me2}$ ($L^{\beta 2} \cdot mmol^{-\beta 2}$)	21.94	14.43
	β_{Me2}	0.926	0.826
	ARE (%)	17.09	18.08
Sheindorf–Rebuhn–Sheintuch isotherm	K_{FMe1} ($L \cdot g^{-1}$)	0.230	0.035
	n_{Me1}	0.029	0.989
	$\alpha_{Me1,Me2}$ ($L \cdot mmol^{-1}$)	1.04	0.931
	K_{FMe2} ($L \cdot g^{-1}$)	1.23	0.753
	n_{Me2}	3.83	1.03
	$\alpha_{Me2,Me1}$ ($L \cdot mmol^{-1}$)	2.33	2.19
	ARE (%)	42.46	40.60

The maximum total metal uptake values, q_{max}, determined by the extended Langmuir model were lower than the sum of the individual $q_{max,Me}$ values obtained by the Langmuir model for the mono-adsorbate systems [18,32,33]. This finding provides further evidence that there are numerous active sites through which both metals can be sequestered and for which they will, to some extent, compete when coexisting in a biadsorbate system. Similar results were obtained by Albadarin and Mangwandi, 2015 [80], who worked with olive stone biomass for the simultaneous removal of Alizarin Red S and Methylene Blue dyes. These conclusions seem to violate the Langmuir isotherm assumptions of a homogeneous sorbent surface and no preferential biosorption or interaction between sorbates. This fact can explain the best fitting results obtained with the Redlich-Peterson and extended Sips isotherms. Both of these models incorporate the isotherm theory of both the Langmuir and Freundlich models.

For the two binary systems studied, b_{Cr} was higher than b_{Zn} and b_{Cd}, indicating that the binding sites of the OW have a higher affinity for chromium than for zinc and cadmium.

Table 4 shows the literature data for binary systems containing at least one of the metals used in this study, together with the results obtained in this research. As can be seen, the maximum adsorption capacities obtained in this study are comparable to those reported in the literature for the adsorption of binary metal mixtures on different adsorbent materials. Furthermore, other researchers have successfully used the same models used in this study to represent the equilibria of metal adsorption in binary systems.

Table 4. Data of binary systems referenced in the bibliography with some of the studied metals.

Binary System	Adsorbent	Maximum Sorption Capacity	Isotherm Model	Ref.
Cr^{3+} Pb^{2+}	*Salvinia natans* macrophyte	0.331 mmol $Cr^{3+}\cdot g^{-1}$ 0.283 mmol $Pb^{2+}.g^{-1}$	Uncompetitive Langmuir model	[81]
Cr^{3+} Zn^{2+}	Dealginated seaweed waste	1.385 mmol $Cr^{3+}\cdot g^{-1}$ 0.489 mmol $Zn^{2+}.g^{-1}$	Langmuir-Freundlich model	[38]
Cr^{3+} Cu^{2+}	*Sargassum* sp.	1.30 mmol $Cr^{3+}\cdot g^{-1}$ 1.08 mmol $Cu^{2+}.g^{-1}$	Freundlich isotherm	[82]
Cd^{2+} Ni^{2+}	NaOH-modified lemon peel.	0.430 mmol $Cd^{2+}.g^{-1}$ 0.447 mmol $Ni^{2+}.g^{-1}$	Langmuir isotherm	[13]
Cu^{2+} Cd^{2+}	Pine bark	0.172 mmol $Cu^{2+}.g^{-1}$ 0.121 mmol $Cd^{2+}.g^{-1}$	Sips isotherm	[78]
Cu^{2+} Cd^{2+}	Water treatment residuals	1.022 mmol $Cu^{2+}.g^{-1}$ 0.693 mmol $Cd^{2+}.g^{-1}$	Langmuir isotherm	[83]
Cu^{2+} Zn^{2+}	Water treatment residuals	1.354 mmol $Cu^{2+}.g^{-1}$ 0.288 mmol $Cd^{2+}.g^{-1}$	Langmuir isotherm	[83]
Zn^{2+} Ni^{2+}	Crab shell biomass	3.07 mmol $Zn^{2+}.g^{-1}$ 3.37 mmol $Ni^{2+}.g^{-1}$	Externded Sips isotherm	[29]
Cr^{3+} Zn^{2+}	Orange waste	0.787 mmol $Cr^{3+}\cdot g^{-1}$ 0.453 mmol $Zn^{2+}.g^{-1}$	Extended Sips isotherm	This work
Cr^{3+} Cd^{2+}	Orange waste	1.096 mmol $Cr^{3+}\cdot g^{-1}$ 0.573 mmol $Cd^{2+}.g^{-1}$	Extended Sips isotherm	This work

One of the most common ways of presenting equilibrium data in biadsorbate systems is through three-dimensional (3D) graphs. These plots are obtained by plotting the adsorption capacity of one adsorbate or the total adsorption capacity against the concentrations of the adsorbates in the solution, once equilibrium has been reached. Therefore, for a biadsorbate system, three plots are obtained, one for the adsorption capacity of each adsorbate and a third one for the total adsorption capacity. In each plot, the adsorption isotherm is represented by a surface. Figures 9 and 10 show, for each of the biadsorbate systems, the experimental equilibrium data (points) together with the adsorption isotherms obtained with the extended Sips model (surfaces), which is the one that best describes the equilibrium data. The competition between metals for adsorption sites and the selectivity of the biosorbent for these metals can be assessed by examining Figures 9 and 10.

The effect of the competitive ion Cd^{2+} or Zn^{2+} can be verified by the slope of the surface observed in the plot of the biosorption capacity of Cr^{3+} ions versus the concentration of the binary solution Cd^{2+}-Cr^{3+} or Zn^{2+}-Cr^{3+} (Figure 9 or Figure 10). The smooth slope of the surface with respect to the Cd^{2+} or Zn^{2+} axis indicates a small influence of these ions on the removal of Cr^{3+} ions. For the two binary systems studied, the plots of chromium biosorption capacity versus metal concentration in the binary solution show a sharp slope of the surface towards the axis of the competing ion (Cd^{2+} or Zn^{2+}). Conse-

quently, at higher concentrations of Cr^{3+}, the removal efficiency for Cd^{2+} or Zn^{2+} ions is strongly reduced.

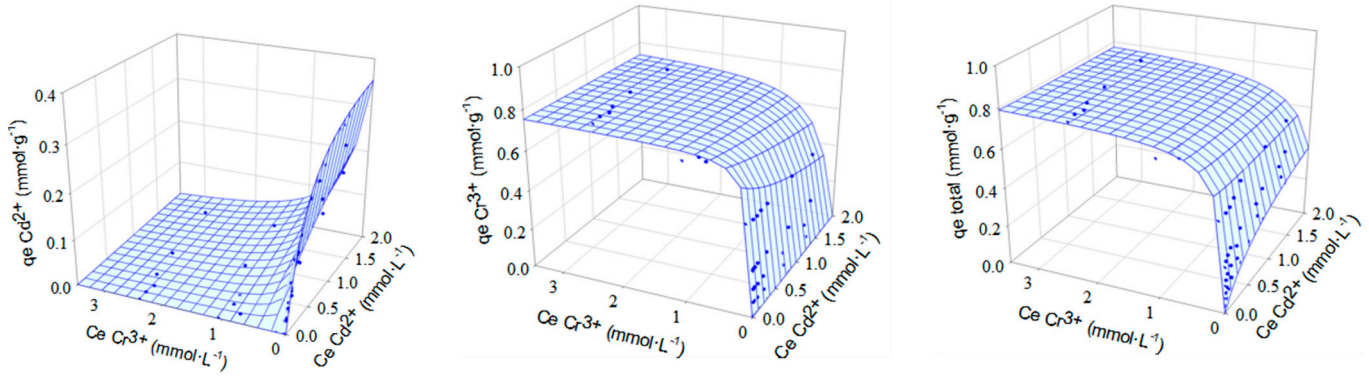

(**a**) (**b**) (**c**)

Figure 9. Isotherms for simultaneous biosorption of Cd^{2+} and Cr^{3+} onto OW. Experimental equilibrium data (•) fitted to the extended Sips model (sorption surfaces). (**a**) $q_{e,Cd}{}^{2+}$; (**b**) $q_{e,Cr}{}^{3+}$ and (**c**) $q_{e,total}$.

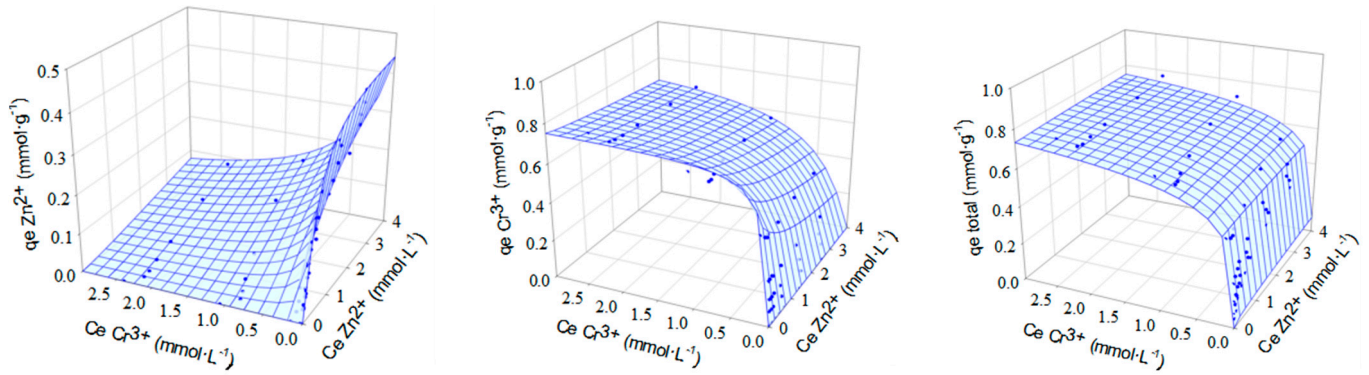

(**a**) (**b**) (**c**)

Figure 10. Isotherms for simultaneous biosorption of Zn^{2+} and Cr^{3+} onto OW. Experimental equilibrium data (•) fitted to the extended Sips model (sorption surfaces). (**a**) $q_{e,Zn}{}^{2+}$; (**b**) $q_{e,Cr}{}^{3+}$ and (**c**) $q_{e,total}$.

4. Conclusions

This research confirms that OW biomass has the potential to be used as a biosorbent for heavy metal removal from aqueous bimetallic solutions, which are more representative of real effluents than mono-adsorbate systems, and underlines the competition between metals for active sites on the surface of the adsorbent.

FTIR spectra of OW showed the complex nature of the biomass. After metals sorption, light shifts in the peak positions at 3422 cm^{-1} (corresponding to hydroxyl groups including adsorbed moisture), 1636 cm^{-1} (corresponding to C=C stretching that can be attributed to the presence of aromatic rings, COO^- asymmetric stretching, and the bending vibration of the interlayer water molecules), and 1431 cm^{-1} (corresponding to C=O in ionic carboxylic groups and to HCH and OCH in plane bending vibration (as in cellulose)) were observed. This pointed out the important role that oxygenated functional groups can play in metal adsorption onto OW, and it can be hypothesized that the main mechanisms of biosoption are surface complexation and ionic exchange. Further studies would be necessary to confirm the adsorption mechanisms involved.

The pH_{pzc} of the biomass (≈5.3) indicate that other mechanisms different to electrostatic attraction, such as ion exchange, must be involved in the sorption of heavy metals onto OW.

The biomass showed a higher selectivity for Cr^{3+} ions than for Cd^{2+} or Zn^{2+} ions. In the presence of Cd^{2+} or Zn^{2+} ions in solution, chromium removal was only slightly affected. Conversely, the presence of Cr^{3+} ions induced a strong reduction in the removal of Cd^{2+} or Zn^{2+}.

A series of multicomponent isotherm models were used to correlate the binary equilibrium data. Both binary systems studied were better represented by the extended Sips isotherm model. Based on this model, the maximum biosorption capacity of OW in the binary system was nearly 0.573 mmol·g^{-1} for Cd^{2+}, 0.453 mmol·g^{-1} for Zn^{2+}, and up to 1.096 mmol·g^{-1} for Cr^{3+}.

Supplementary Materials: The following supporting information can be downloaded at: https://www.mdpi.com/article/10.3390/pr12010148/s1, Figure S1: Dependence of the relative biosorption of metal i on the initial concentrations of metals i and k. (a) Metal i = Zn^{2+} and metal k = Cr^{3+}, (b) metal i = Cr^{3+} and metal k = Zn^{2+}. Figure S2. Dependence of the biosorption efficiency of metal i on the initial concentrations of metals i and k. (a) Metal i = Zn^{2+} and metal k = Cr^{3+}, (b) metal i = Cr^{3+} and metal k = Zn^{2+}. Figure S3. Dependence of the relative coverage of metal i on the initial concentrations of metals i and k. (a) Metal i = Zn^{2+} and metal k = Cr^{3+}, (b) metal i = Cr^{3+} and metal k = Zn^{2+}.

Author Contributions: Conceptualization, A.B.P.-M., J.F.O., M.I.A., M.L. and V.F.M.; methodology, A.B.P.-M., J.F.O., M.I.A., M.L. and V.F.M.; software, A.B.P.-M., J.F.O., M.I.A., M.L. and V.F.M.; validation, A.B.P.-M., J.F.O., M.I.A., M.L. and V.F.M.; formal analysis, A.B.P.-M., J.F.O., M.I.A., M.L. and V.F.M.; investigation, A.B.P.-M., J.F.O., M.I.A., M.L. and V.F.M.; resources, A.B.P.-M., J.F.O., M.I.A., M.L. and V.F.M.; data curation, A.B.P.-M., J.F.O., M.I.A., M.L. and V.F.M.; writing—original draft preparation, A.B.P.-M., J.F.O., M.I.A., M.L. and V.F.M.; writing—review and editing, A.B.P.-M., J.F.O., M.I.A., M.L. and V.F.M. All authors have read and agreed to the published version of the manuscript.

Funding: This research received no external funding.

Data Availability Statement: The data presented in this study are available on request from the corresponding author.

Conflicts of Interest: The authors declare no conflicts of interest.

References

1. Yan, A.; Wang, Y.; Tan, S.N.; Mohd Yusof, M.L.; Ghosh, S.; Chen, Z. Phytoremediation: A Promising Approach for Revegetation of Heavy Metal-Polluted Land. *Front. Plant Sci.* **2020**, *11*, 513099. [CrossRef] [PubMed]
2. Mohan, D.; Pittman, C.U. Activated Carbons and Low Cost Adsorbents for Remediation of Tri- and Hexavalent Chromium from Water. *J. Hazard. Mater.* **2006**, *137*, 762–811. [CrossRef] [PubMed]
3. Ozbey, E.; Asma, D. Chromium (III) Biosorption of Deinococcus Radiodurans and Its Vitreoscilla Haemoglobin (Vgb) Gene-Transferred Recombinants. *J. Pharm. Pharmacol.* **2021**, *9*, 140–148. [CrossRef]
4. De Zuane, J. *Handbook of Drinking Water Quality*; John Wiley & Sons: Hoboken, NJ, USA, 1996. [CrossRef]
5. Cheung, C.W.; Porter, J.F.; Mckay, G. Sorption Kinetic Analysis for the Removal of Cadmium Ions from Effluents Using Bone Char. *Water Res.* **2001**, *35*, 605–612. [CrossRef] [PubMed]
6. Miretzky, P.; Cirelli, A.F. Cr(VI) and Cr(III) Removal from Aqueous Solution by Raw and Modified Lignocellulosic Materials: A Review. *J. Hazard. Mater.* **2010**, *180*, 1–19. [CrossRef] [PubMed]
7. Ortiz-Quiñonez, J.L.; Cancino-Gordillo, F.E.; Pal, U. Removal of Cr(III) Ions from Water Using Magnetically Separable Graphene-Oxide-Decorated Nickel Ferrite Nanoparticles. *ACS Appl. Nano Mater.* **2023**, *6*, 18491–18507. [CrossRef]
8. United Nations Water and Sanitation—United Nations Sustainable Development. Available online: https://www.un.org/sustainabledevelopment/water-and-sanitation/ (accessed on 7 December 2023).
9. Šćiban, M.; Radetić, B.; Kevrešan, Ž.; Klašnja, M. Adsorption of Heavy Metals from Electroplating Wastewater by Wood Sawdust. *Bioresour. Technol.* **2007**, *98*, 402–409. [CrossRef]
10. Ofomaja, A.E.; Unuabonah, E.I.; Oladoja, N.A. Competitive Modeling for the Biosorptive Removal of Copper and Lead Ions from Aqueous Solution by Mansonia Wood Sawdust. *Bioresour. Technol.* **2010**, *101*, 3844–3852. [CrossRef]

11. Madadgar, S.; Doulati Ardejani, F.; Boroumand, Z.; Sadeghpour, H.; Taherdangkoo, R.; Butscher, C. Biosorption of Aqueous Pb(II), Co(II), Cd(II) and Ni(II) Ions from Sungun Copper Mine Wastewater by Chrysopogon Zizanioides Root Powder. *Minerals* **2023**, *13*, 106. [CrossRef]
12. Fomina, M.; Gadd, G.M. Biosorption: Current Perspectives on Concept, Definition and Application. *Bioresour. Technol.* **2014**, *160*, 3–14. [CrossRef]
13. Villen-Guzman, M.; Cerrillo-Gonzalez, M.M.; Paz-Garcia, J.M.; Rodriguez-Maroto, J.M.; Arhoun, B. Valorization of Lemon Peel Waste as Biosorbent for the Simultaneous Removal of Nickel and Cadmium from Industrial Effluents. *Environ. Technol. Innov.* **2021**, *21*, 101380. [CrossRef]
14. Banerjee, M.; Basu, R.K.; Das, S.K. Cu(II) Removal Using Green Adsorbents: Kinetic Modeling and Plant Scale-up Design. *Environ. Sci. Pollut. Res.* **2019**, *26*, 11542–11557. [CrossRef] [PubMed]
15. Karić, N.; Maia, A.S.; Teodorović, A.; Atanasova, N.; Langergraber, G.; Crini, G.; Ribeiro, A.R.L.; Đolić, M. Bio-Waste Valorisation: Agricultural Wastes as Biosorbents for Removal of (in)Organic Pollutants in Wastewater Treatment. *Chem. Eng. J. Adv.* **2022**, *9*, 100239. [CrossRef]
16. Šoštarić, T.; Petrović, M.; Milojković, J.; Lačnjevac, Č.; Ćosović, A.; Stanojević, M.; Stojanović, M. Application of Apricot Stone Waste from Fruit Processing Industry in Environmental Cleanup Copper Biosorption Study. *Fruits* **2015**, *70*, 271–280. [CrossRef]
17. Amer, H.; El-Gendy, A.; El-Haggar, S. Removal of Lead (II) from Aqueous Solutions Using Rice Straw. *Water Sci. Technol.* **2017**, *76*, 1011–1021. [CrossRef] [PubMed]
18. Perez Marin, A.B.; Aguilar, M.I.; Meseguer, V.F.; Ortuno, J.F.; Saez, J.; Llorens, M. Biosorption of Chromium (III) by Orange (Citrus Cinensis) Waste: Batch and Continuous Studies. *Chem. Eng. J.* **2009**, *155*, 199–206. [CrossRef]
19. Yi, Z.J.; Yao, J.; Kuang, Y.F.; Chen, H.L.; Wang, F.; Yuan, Z.M. Removal of Pb(II) by Adsorption onto Chinese Walnut Shell Activated Carbon. *Water Sci. Technol.* **2015**, *72*, 983–989. [CrossRef]
20. Lavado-Meza, C.; De la Cruz-Cerrón, L.; Cisneros-Santos, G.; De la Cruz, A.H.; Angeles-Suazo, J.; Dávalos-Prado, J.Z. Arabica-Coffee and Teobroma-Cocoa Agro-Industrial Waste Biosorbents, for Pb(II) Removal in Aqueous Solutions. *Environ. Sci. Pollut. Res.* **2023**, *30*, 2991–3001. [CrossRef]
21. Mohamed, R.M.; Hashim, N.; Abdullah, S.; Abdullah, N.; Mohamed, A.; Asshaary Daud, M.A.; Aidil Muzakkar, K.F. Adsorption of Heavy Metals on Banana Peel Bioadsorbent. *J. Phys. Conf. Ser.* **2020**, *1532*, 012014. [CrossRef]
22. Afolabi, F.O.; Musonge, P.; Bakare, B.F. Bio-Sorption of Copper and Lead Ions in Single and Binary Systems onto Banana Peels. *Cogent Eng.* **2021**, *8*, 1886730. [CrossRef]
23. Do Nascimento Júnior, W.J.; Landers, R.; Gurgel Carlos Da Silva, M.; Vieira, M.G.A. Equilibrium and Desorption Studies of the Competitive Binary Biosorption of Silver(I) and Copper(II) Ions on Brown Algae Waste. *J. Environ. Chem. Eng.* **2021**, *9*, 104840. [CrossRef]
24. Bayuo, J.; Rwiza, M.J.; Sillanpää, M.; Mtei, K.M. Removal of Heavy Metals from Binary and Multicomponent Adsorption Systems Using Various Adsorbents—A Systematic Review. *RSC Adv.* **2023**, *13*, 13052–13093. [CrossRef] [PubMed]
25. Mahamadi, C. On the Dominance of Pb during Competitive Biosorption from Multi-Metal Systems: A Review. *Cogent Environ. Sci.* **2019**, *5*, 1635335. [CrossRef]
26. Aksu, Z.; Isoglu, I.A. Use of Dried Sugar Beet Pulp for Binary Biosorption of Gemazol Turquoise Blue-G Reactive Dye and Copper(II) Ions: Equilibrium Modeling. *Chem. Eng. J.* **2007**, *127*, 177–188. [CrossRef]
27. Monteiro, C.M.; Castro, P.M.L.; Malcata, F.X. Capacity of Simultaneous Removal of Zinc and Cadmium from Contaminated Media, by Two Microalgae Isolated from a Polluted Site. *Environ. Chem. Lett.* **2011**, *9*, 511–517. [CrossRef]
28. Hammaini, A.; González, F.; Ballester, A.; Blázquez, M.L.; Muñoz, J.A. Simultaneous Uptake of Metals by Activated Sludge. *Miner. Eng.* **2003**, *16*, 723–729. [CrossRef]
29. Morales-Barrera, L.; Cristiani-Urbina, E. Equilibrium Biosorption of Zn2+ and Ni2+ Ions from Monometallic and Bimetallic Solutions by Crab Shell Biomass. *Processes* **2022**, *10*, 886. [CrossRef]
30. Morales-Barrera, L.; Flores-Ortiz, C.M.; Cristiani-Urbina, E. Single and Binary Equilibrium Studies for Ni2+ and Zn2+ Biosorption onto Lemna Gibba from Aqueous Solutions. *Processes* **2020**, *8*, 1089. [CrossRef]
31. Chong, K.H.; Volesky, B. Metal Biosorption Equilibria in a Ternary System. *Biotechnol. Bioeng.* **1996**, *49*, 629–638. [CrossRef]
32. Perez-Marin, A.B.; Zapata, V.M.; Ortuno, J.F.; Aguilar, M.; Saez, J.; Llorens, M. Removal of Cadmium from Aqueous Solutions by Adsorption onto Orange Waste. *J. Hazard. Mater.* **2007**, *139*, 122–131. [CrossRef]
33. Perez Marin, A.B.; Isabel Aguilar, M.; Francisco Ortuno, J.; Francisco Meseguer, V.; Saez, J.; Llorens, A. Biosorption of Zn(II) by Orange Waste in Batch and Packed-Bed Systems. *J. Chem. Technol. Biotechnol.* **2010**, *85*, 1310–1318. [CrossRef]
34. Perez Marin, A.B.; Ortuno, J.F.; Aguilar, M.I.; Meseguer, V.F.; Saez, J.; Llorens, M. Use of Chemical Modification to Determine the Binding of Cd(II), Zn(II) and Cr(III) Ions by Orange Waste. *Biochem. Eng. J.* **2010**, *53*, 2–6. [CrossRef]
35. Fiol, N.; Villaescusa, I. Determination of Sorbent Point Zero Charge: Usefulness in Sorption Studies. *Environ. Chem. Lett.* **2009**, *7*, 79–84. [CrossRef]
36. Sag, Y.; Akcael, B. Multi-Metal Biosorption Equilibria of Cr (VI), Cu (II), Cd (II), and Fe (III) Ions. *Eur. J. Miner. Process. Environ. Prot.* **2002**, *2*, 232–245.
37. Abdulaziz, M.; Musayev, S. Multicomponent Biosorption of Heavy Metals from Aqueous Solutions: A Review. *Pol. J. Environ. Stud.* **2017**, *26*, 1433–1441. [CrossRef] [PubMed]

38. Costa, C.S.D.; Queiroz, B.G.M.; Landers, R.; da Silva, M.G.C.; Vieira, M.G.A. Equilibrium Study of Binary Mixture Biosorption of Cr(III) and Zn(II) by Dealginated Seaweed Waste: Investigation of Adsorption Mechanisms Using X-Ray Photoelectron Spectroscopy Analysis. *Environ. Sci. Pollut. Res.* **2019**, *26*, 28470–28480. [CrossRef] [PubMed]
39. Moreira, V.R.; Lebron, Y.A.R.; Lange, L.C.; Santos, L.V.S. Simultaneous Biosorption of Cd(II), Ni(II) and Pb(II) onto a Brown Macroalgae Fucus Vesiculosus: Mono- and Multi-Component Isotherms, Kinetics and Thermodynamics. *J. Environ. Manag.* **2019**, *251*, 109587. [CrossRef]
40. Terdputtakun, A.; Arqueropanyo, O.; Sooksamiti, P.; Janhom, S.; Naksata, W. Adsorption Isotherm Models and Error Analysis for Single and Binary Adsorption of Cd(II) and Zn(II) Using Leonardite as Adsorbent. *Environ. Earth Sci.* **2017**, *76*, 1–11. [CrossRef]
41. Amrutha; Jeppu, G.; Girish, C.R.; Prabhu, B.; Mayer, K. Multi-Component Adsorption Isotherms: Review and Modeling Studies. *Environ. Process.* **2023**, *10*, 38. [CrossRef]
42. Marquardt, D.W. An Algorithm for Least-Squares Estimation of Nonlinear Parameters. *J. Soc. Ind. Appl. Math.* **1963**, *11*, 431–441. [CrossRef]
43. Al-Ghouti, M.A.; Da'ana, D.A. Guidelines for the Use and Interpretation of Adsorption Isotherm Models: A Review. *J. Hazard. Mater.* **2020**, *393*, 122383. [CrossRef] [PubMed]
44. Hadjiivanov, K. Identification and Characterization of Surface Hydroxyl Groups by Infrared Spectroscopy. In *Advances in Catalysis*; Academic Press: Cambridge, MA, USA, 2014; pp. 99–318.
45. Shabanian, M.; Hajibeygi, M.; Raeisi, A. FTIR Characterization of Layered Double Hydroxides and Modified Layered Double Hydroxides. In *Layered Double Hydroxide Polymer Nanocomposites*; Elsevier: Amsterdam, The Netherlands, 2020; pp. 77–101.
46. Feng, N.; Guo, X.; Liang, S.; Zhu, Y.; Liu, J. Biosorption of Heavy Metals from Aqueous Solutions by Chemically Modified Orange Peel. *J. Hazard. Mater.* **2011**, *185*, 49–54. [CrossRef] [PubMed]
47. Arslanoglu, H.; Soner Altundogan, H.; Tumen, F. Preparation of Cation Exchanger from Lemon and Sorption of Divalent Heavy Metals. *Bioresour. Technol.* **2008**, *99*, 2699–2705. [CrossRef] [PubMed]
48. Lasheen, M.R.; Ammar, N.S.; Ibrahim, H.S. Adsorption/Desorption of Cd(II), Cu(II) and Pb(II) Using Chemically Modified Orange Peel: Equilibrium and Kinetic Studies. *Solid State Sci.* **2012**, *14*, 202–210. [CrossRef]
49. Feng, N.; Guo, X.; Liang, S. Adsorption Study of Copper (II) by Chemically Modified Orange Peel. *J. Hazard. Mater.* **2009**, *164*, 1286–1292. [CrossRef]
50. Sari, A.; Mendil, D.; Tuzen, M.; Soylak, M. Biosorption of Cd(II) and Cr(III) from Aqueous Solution by Moss (Hylocomium Splendens) Biomass: Equilibrium, Kinetic and Thermodynamic Studies. *Chem. Eng. J.* **2008**, *144*, 1–9. [CrossRef]
51. Chakravarty, S.; Bhattacharjee, S.; Gupta, K.K.; Singh, M.; Chaturvedi, H.T.; Maity, S. Adsorption of Zinc from Aqueous Solution Using Chemically Treated Newspaper Pulp. *Bioresour. Technol.* **2007**, *98*, 3136–3141. [CrossRef]
52. Akinhanmi, T.F.; Ofudje, E.A.; Adeogun, A.I.; Aina, P.; Joseph, I.M. Orange Peel as Low-Cost Adsorbent in the Elimination of Cd(II) Ion: Kinetics, Isotherm, Thermodynamic and Optimization Evaluations. *Bioresour. Bioprocess.* **2020**, *7*, 34. [CrossRef]
53. Cai, Y.; Jiang, W.; Liu, D.; Chang, C. Adsorption of Sulfanilamides Using Biochar Derived from Suaeda Salsa: Adsorption Kinetics, Isotherm, Thermodynamics, and Mechanism. *Environ. Sci. Pollut. Res.* **2023**, *7*, 34. [CrossRef]
54. De Carvalho, H.P.; Huang, J.; Zhao, M.; Liu, G.; Dong, L.; Liu, X. Improvement of Methylene Blue Removal by Electrocoagulation/Banana Peel Adsorption Coupling in a Batch System. *Alex. Eng. J.* **2015**, *54*, 777–786. [CrossRef]
55. Ellerbrock, R.H.; Gerke, H.H. FTIR Spectral Band Shifts Explained by OM–Cation Interactions. *J. Plant Nutr. Soil Sci.* **2021**, *184*, 388–397. [CrossRef]
56. Kratochvil, D.; Volesky, B. Advances in the Biosorption of Heavy Metals. *Trends Biotechnol.* **1998**, *16*, 291–300. [CrossRef]
57. Gérente, C.; Couespel Du Mesnil, P.; Andrès, Y.; Thibault, J.F.; Le Cloirec, P. Removal of Metal Ions from Aqueous Solution on Low Cost Natural Polysaccharides: Sorption Mechanism Approach. *React. Funct. Polym.* **2000**, *46*, 135–144. [CrossRef]
58. Dupont, L.; Bouanda, J.; Ghanbaja, J.; Dumonceau, J.; Aplincourt, M. Use of Analytical Microscopy to Analyze the Speciation of Copper and Chromium Ions onto a Low-Cost Biomaterial. *J. Colloid Interface Sci.* **2004**, *279*, 418–424. [CrossRef] [PubMed]
59. Panda, G.C.; Das, S.K.; Chatterjee, S.; Maity, P.B.; Bandopadhyay, T.S.; Guha, A.K. Adsorption of Cadmium on Husk of Lathyrus Sativus: Physico-Chemical Study. *Colloids Surf. B Biointerfaces* **2006**, *50*, 49–54. [CrossRef] [PubMed]
60. Cholico-González, D.; Ortiz Lara, N.; Fernández Macedo, A.M.; Chavez Salas, J. Adsorption Behavior of Pb(II), Cd(II), and Zn(II) onto Agave Bagasse, Characterization, and Mechanism. *ACS Omega* **2020**, *5*, 3302–3314. [CrossRef]
61. Lavado-Meza, C.; Fernandez-Pezua, M.C.; Gamarra-Gómez, F.; Sacari-Sacari, E.; Angeles-Suazo, J.; Dávalos-Prado, J.Z. Single and Binary Removals of Pb(II) and Cd(II) with Chemically Modified Opuntia Ficus Indica Cladodes. *Molecules* **2023**, *28*, 4451. [CrossRef]
62. Zhu, S.; Khan, M.A.; Wang, F.; Bano, Z.; Xia, M. Exploration of Adsorption Mechanism of 2-Phosphonobutane-1,2,4-Tricarboxylic Acid onto Kaolinite and Montmorillonite via Batch Experiment and Theoretical Studies. *J. Hazard. Mater.* **2021**, *403*, 123810. [CrossRef]
63. Esfandiar, N.; Suri, R.; McKenzie, E.R. Competitive Sorption of Cd, Cr, Cu, Ni, Pb and Zn from Stormwater Runoff by Five Low-Cost Sorbents; Effects of Co-Contaminants, Humic Acid, Salinity and PH. *J. Hazard. Mater.* **2022**, *423*, 126938. [CrossRef]
64. Ambaye, T.G.; Vaccari, M.; van Hullebusch, E.D.; Amrane, A.; Rtimi, S. Mechanisms and Adsorption Capacities of Biochar for the Removal of Organic and Inorganic Pollutants from Industrial Wastewater. *Int. J. Environ. Sci. Technol.* **2021**, *18*, 3273–3294. [CrossRef]

65. Yang, X.; Wan, Y.; Zheng, Y.; He, F.; Yu, Z.; Huang, J.; Wang, H.; Ok, Y.S.; Jiang, Y.; Gao, B. Surface Functional Groups of Carbon-Based Adsorbents and Their Roles in the Removal of Heavy Metals from Aqueous Solutions: A Critical Review. *Chem. Eng. J.* **2019**, *366*, 608–621. [CrossRef] [PubMed]
66. Kim, D.S. The Removal by Crab Shell of Mixed Heavy Metal Ions in Aqueous Solution. *Bioresour. Technol.* **2003**, *87*, 355–357. [CrossRef] [PubMed]
67. Ma, W.; Tobin, J.M. Development of Multimetal Binding Model and Application to Binary Metal Biosorption onto Peat Biomass. *Water Res.* **2003**, *37*, 3967–3977. [CrossRef] [PubMed]
68. Mahamadi, C.; Nharingo, T. Competitive Adsorption of Pb2+, Cd2+ and Zn2+ Ions onto Eichhornia Crassipes in Binary and Ternary Systems. *Bioresour. Technol.* **2010**, *101*, 859–864. [CrossRef] [PubMed]
69. Jain, M.; Garg, V.K.; Kadirvelu, K.; Sillanpää, M. Adsorption of Heavy Metals from Multi-Metal Aqueous Solution by Sunflower Plant Biomass-Based Carbons. *Int. J. Environ. Sci. Technol.* **2016**, *13*, 493–500. [CrossRef]
70. Park, J.H.; Ok, Y.S.; Kim, S.H.; Cho, J.S.; Heo, J.S.; Delaune, R.D.; Seo, D.C. Competitive Adsorption of Heavy Metals onto Sesame Straw Biochar in Aqueous Solutions. *Chemosphere* **2016**, *142*, 77–83. [CrossRef]
71. Yang, S.; Xiao, X.; Tao, E. Removing Low Concentration of Cr (III) from Wastewater: Using Titanium Dioxide Surface Modified Montmorillonite as a Selective Adsorbent. *Inorg. Chem. Commun.* **2021**, *125*, 108464. [CrossRef]
72. Persson, I. Hydrated Metal Ions in Aqueous Solution: How Regular Are Their Structures? *Pure Appl. Chem.* **2010**, *82*, 1901–1917. [CrossRef]
73. Han, H.; Rafiq, M.K.; Zhou, T.; Xu, R.; Mašek, O.; Li, X. A Critical Review of Clay-Based Composites with Enhanced Adsorption Performance for Metal and Organic Pollutants. *J. Hazard. Mater.* **2019**, *369*, 780–796. [CrossRef]
74. Figueira, M.M.; Volesky, B.; Ciminelli, V.S.T. Assessment of Interference in Biosorption of a Heavy Metal. *Biotechnol. Bioeng.* **1997**, *54*, 344–350. [CrossRef]
75. Pagnanelli, F.; Trifoni, M.; Beolchini, F.; Esposito, A.; Toro, L.; Vegliò, F. Equilibrium Biosorption Studies in Single and Multi-Metal Systems. *Process Biochem.* **2001**, *37*, 115–124. [CrossRef]
76. Villaescusa, I.; Fiol, N.; Martínez, M.; Miralles, N.; Poch, J.; Serarols, J. Removal of Copper and Nickel Ions from Aqueous Solutions by Grape Stalks Wastes. *Water Res.* **2004**, *38*, 992–1002. [CrossRef] [PubMed]
77. Srivastava, V.C.; Mall, I.D.; Mishra, I.M. Equilibrium Modelling of Single and Binary Adsorption of Cadmium and Nickel onto Bagasse Fly Ash. *Chem. Eng. J.* **2006**, *117*, 79–91. [CrossRef]
78. Al-Asheh, S.; Banat, F.; Al-Omari, R.; Duvnjak, Z. Predictions of Binary Sorption Isotherms for the Sorption of Heavy Metals by Pine Bark Using Single Isotherm Data. *Chemosphere* **2000**, *41*, 659–665. [CrossRef] [PubMed]
79. Ayawei, N.; Ebelegi, A.N.; Wankasi, D. Modelling and Interpretation of Adsorption Isotherms. *J. Chem.* **2017**, *2017*, 3039817. [CrossRef]
80. Albadarin, A.B.; Mangwandi, C. Mechanisms of Alizarin Red S and Methylene Blue Biosorption onto Olive Stone By-Product: Isotherm Study in Single and Binary Systems. *J. Environ. Manag.* **2015**, *164*, 86–93. [CrossRef] [PubMed]
81. Lima, L.K.S.; Silva, M.G.C.; Vieira, M.G.A. Study of Binary and Single Biosorption by the Floating Aquatic Macrophyte Salvinia Natans. *Braz. J. Chem. Eng.* **2016**, *33*, 649–660. [CrossRef]
82. Silva, E.A.; Cossich, E.S.; Tavares, C.G.; Cardozo Filho, L.; Guirardello, R. Biosorption of Binary Mixtures of Cr(III) and Cu(II) Ions by *Sargassum* sp. *Braz. J. Chem. Eng.* **2003**, *20*, 213–227. [CrossRef]
83. Duan, R.; Fedler, C.B. Competitive Adsorption of Cu^{2+}, Pb^{2+}, Cd^{2+}, and Zn^{2+} onto Water Treatment Residuals: Implications for Mobility in Stormwater Bioretention Systems. *Water Sci. Technol.* **2022**, *86*, 878–893. [CrossRef]